Simulating Electrochemical Systems by Combining the Finite Field Method with a Constant Potential Electrode

Thomas Dufils,[1] Guillaume Jeanmairet⬤,[1] Benjamin Rotenberg⬤,[1] Michiel Sprik,[2] and Mathieu Salanne⬤[1,*]

[1]*Sorbonne Université, CNRS, Physico-chimie des Électrolytes et Nanosystèmes Interfaciaux, PHENIX, F-75005 Paris, France*
[2]*Department of Chemistry, University of Cambridge, Cambridge CB2 1EW, United Kingdom*

A better understanding of interfacial mechanisms is needed to improve the performances of electrochemical devices. Yet, simulating an electrode surface at fixed electrolyte composition remains a challenge. Here, we apply a finite electric field to a single electrode held at constant potential and in contact with an aqueous ionic solution, using classical molecular dynamics. The polarization yields two electrochemical interfaces on opposite sides of the same metal slab. The net charge on one electrode surface is the opposite of the net charge on the other, maintaining overall charge neutrality of the metal. The electrode surface charge fluctuations are compensated by the adsorption of ions from the electrolyte, forming a pair of electric double layers with aligned dipoles. This opens the way towards the efficient simulation of electrochemical interfaces using any flavor of molecular dynamics, from classical to first-principles-based methods.

Despite many advances over the past decades [1,2], the efficient simulation of full electrochemical cells at the molecular scale, using electronic structure based calculations, remains a daunting task. This is due to their slab structure, since the minimal experimental setup consists of an electrolyte between two electrodes. The system is generally simplified by simulating one interface only, but the main conceptual difficulty is to find a way to charge the electrode surface at fixed composition of the electrolyte. Several methods have recently emerged [3–5], where the system is allowed to exchange electrons with a reservoir at fixed voltage (grand-canonical approach), but they all rely on the use of continuum descriptions for the electrolyte. These models, which are generally based on a Poisson-Boltzmann theory [6], remain mostly qualitative and an atomistic description would be preferable (this is also true because the solvent may actively participate to electrochemical reactions [7,8]). This is almost impossible to do since it would be necessary to remove or insert ions to counterbalance the electrode charge fluctuations.

Here, we propose an alternative route to simulate electrochemical cells. Our approach is based on the coupling of a finite field with a system consisting in an electrolyte and a single electrode. Finite field methods, developed in the framework of the modern theory of polarization, consist of imposing a macroscopic field (electric field [9], polarization [10], or electric displacement [11]) via an extended Hamiltonian accounting for the interaction between the system and the fixed field. They have recently been adapted and applied to the study of electrical double layers at solid-liquid interfaces, and more precisely charged [12] or polar [13] insulator-electrolyte

interfaces. Electrochemical systems are by nature more complex since they involve metallic electrodes whose charge distribution is not fixed but depends on the surrounding medium and the applied potential. Because of the long simulation times related to the relaxation of the electrical double layer (which is typically longer than the nanosecond), we establish here a proof of concept by using a classical molecular dynamics (MD) setup. Indeed, even if metals can only be accurately described in the framework of quantum mechanics, models have been developed to reproduce the electrostatics in classical or mixed quantum and classical simulations [14,15]. In this contribution we extend the finite electric field method to an electrolyte interacting with such a model metallic electrode.

In the following, we focus on the description of the electrostatics, the van der Waals interactions being represented by the conventional Lennard-Jones model. The charge density in any point of space is given by

$$\rho(\mathbf{r}) = \sum_{i=1}^{N} q_i \delta(\mathbf{r} - \mathbf{r}_i) + \sum_{j=1}^{M} q_j \eta^3 \pi^{3/2} \exp\left[-\eta^2 (\mathbf{r} - \mathbf{r}_j)^2\right],$$

(1)

where the first term is the contribution of the electrolyte, represented by a distribution of point charges with q_i the partial charge of the atom $i \in [1, N]$ and $\mathbf{r}_i$ its position; δ is the Dirac distribution. The second term represents the atoms of the metallic electrode, in which each site $j \in [1, M]$ is immobile (with position $\mathbf{r}_j$) and carries a charge q_j which is spatially distributed following a Gaussian charge distribution of width η^{-1}. In order to represent the metallic

character of the electrodes, the latter charges are allowed to fluctuate in response to the electrolyte fluctuations and thus are part of the microscopic degrees of freedom [14,16]. The Hamiltonian of the system is written as

$$H^{\mathrm{PBC}} = K(\mathbf{p}^N) + U(\mathbf{r}^N, \mathbf{q}^M), \qquad (2)$$

where $K(\mathbf{p}^N)$ is the kinetic energy which depends on the ion momenta $\mathbf{p}^N = \{\mathbf{p}_1, ..., \mathbf{p}_N\}$ and $U(\mathbf{r}^N, \mathbf{q}^M)$ the potential energy, which depends on the ion positions $\mathbf{r}^N = \{\mathbf{r}_1, ..., \mathbf{r}_N\}$ and charges of the electrode $\mathbf{q}^M = \{q_1, ..., q_M\}$. We have appended a superscript PBC (periodic boundary conditions) to indicate that the electrostatic energies and forces are computed using the standard Ewald summation technique. All the atoms within an electrode are held at constant potential by enforcing the following condition on each atom:

$$\Psi_j^{\mathrm{PBC}} = \frac{\partial U_C^{\mathrm{PBC}}}{\partial q_j} = \Psi_J, \qquad (3)$$

where Ψ_J is the prescribed potential of electrode J to which the atom j belongs and U_C^{PBC} is the Coulombic contribution to the energy, given by

$$U_C^{\mathrm{PBC}} = \frac{1}{2} \iint \frac{\rho(\mathbf{r})\rho(\mathbf{r}')}{4\pi\epsilon_0|\mathbf{r} - \mathbf{r}'|} d\mathbf{r}d\mathbf{r}'. \qquad (4)$$

Note that this expression will contain a self energy for the interaction of each Gaussian charge density with itself only (it is omitted for the point charges).

Formally, solving the set of self-consistent equations given by Eq. (3) is equivalent to minimizing $U_C^{\mathrm{PBC}} - \sum_j \Psi_J q_j$ with respect to the charges. Since this function is quadratic in the fluctuating charges q_j [see Eq. (4)], the minimization can be efficiently performed with conjugate gradients. Note that we add an additional constraint by forcing the sum of the electrode charges to be null [17].

The minimal components of an electrochemical cell are two electrodes and an electrolyte between them. In classical MD, the computational cost is not prohibitive so it is relatively easy to simulate complete systems instead of a single electrode surface. The conventional setup to simulate such systems is illustrated in the top panel of Fig. 1. In the following, we will refer to this system as the electrolyte-centered supercell (ECS). It is simulated using the 2D Ewald summation [18,19] since the two electrodes are held at different potentials ($\Psi_J = \Psi_{\mathrm{left}}$ or Ψ_{right}). We note x and y the two directions along which PBCs are used in this setup.

Finite field (**E**) simulations can be performed using the extended Hamiltonian introduced by Stengel et al. in Ref. [11] and is written as

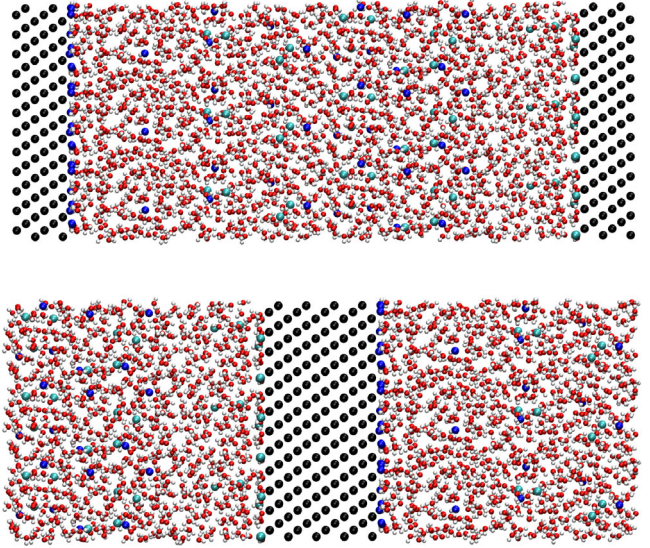$$H_E = H^{\mathrm{PBC}} - \Omega \mathbf{P} \cdot \mathbf{E}, \qquad (5)$$

FIG. 1. Top: electrolyte-centered supercell (2D PBCs), with fixed applied potential between two electrodes ($\Delta\Psi = \Psi_{\mathrm{right}} - \Psi_{\mathrm{left}}$). Bottom: conductor-centered supercell (3D PBCs), with a finite field **E** and a single electrode in which the potential of the atoms is set to the same value $\Psi_{\mathrm{electrode}}$.

where H^{PBC} is the Hamiltonian defined by Eq. (2), Ω is the volume of the supercell, and **P** the polarization per unit volume. In the modern theory of polarization, the dipole moment of a unit cell involving infinite periodic systems is viewed as a multivalued quantity, since it depends on the choice of the position of the periodic boundaries. Nevertheless, this is not a significant issue since only differences in polarization matter in the dynamics and in the calculation of physical properties, in practice via the itinerant polarization [20]:

$$\mathbf{P}_{\mathrm{itinerant}}(t) = \mathbf{P}_{\mathrm{itinerant}}(0) + \frac{1}{\Omega} \sum_{i=1}^{N} q_i \Delta\mathbf{r}_i(t), \qquad (6)$$

where $\Delta\mathbf{r}_i$ is the displacement of the atom between time $t = 0$ and t for the "unfolded" trajectory, i.e., not taking jumps in position (hence polarization) across the periodic boundaries. The system must be periodic in the direction in which the finite electric field is applied, which implies the use of 3D PBCs. A field E corresponds to a drop of Poisson potential across the cell $\Delta\Psi = -EL_z$, where L_z is the length of the box (and not the distance between the two electrode surfaces) in the direction of the field. From the practical point of view, a consequence of the use of 3D PBCs is that now the two electrodes of the ECS necessarily merge, yielding a single electrode at fixed potential $\Psi_J = \Psi_{\mathrm{electrode}}$. The simulation cell can then be represented with the electrode at its center, yielding the conductor-centered supercell (CCS) shown in the bottom panel of Fig. 1. Contrarily to the constant applied potential simulations, it is now the presence of the finite field that induces the

polarization of the electrode and potential drop at the two electrode-electrolyte interfaces.

Coupling fluctuating charges to model conductors with finite field simulations requires two important adaptations of both methods. On the one hand, the cell polarization includes a contribution from the fluctuating charges as

$$\mathbf{P}_{\text{conductor}}(t) = \frac{1}{\Omega} \sum_{j=1}^{M} q_j(t)\mathbf{r}_j. \tag{7}$$

This additional term does not depend on the position of the electrode inside the supercell since we enforce $\sum_j q_j = 0$. On the other hand, the determination of the partial charges via the constraint of fixed potential includes an additional contribution to the electrostatic energy and potential due to the finite field. From the extended Hamiltonian [Eq. (5)] and the expression of the electrode contribution to polarization [Eq. (7)], one obtains the generalization of Eq. (3) as

$$\Psi_j = \Psi_j^{\text{PBC}} - \mathbf{r}_j \cdot \mathbf{E} = \Psi_J. \tag{8}$$

As an extension of the constant applied potential case, the self-consistent expressions given by Eq. (8) are now solved by minimizing $U_C^{\text{PBC}} - \Omega\mathbf{P} \cdot \mathbf{E} - \sum_j \Psi_J q_j$ with

respect to the charges. Since **P** is a linear function of the charges, the performances of the conjugate gradient minimizer are not affected by this setup.

In order to test this new approach, we simulate two systems, one at constant applied potential between two distinct electrodes and the other with the finite field method and a single fixed-potential electrode as shown on Fig. 1. The electrode(s) consist of a model structure made of a cubic crystal with the NaCl lattice constant, with the (111) plane facing the liquid. The intermolecular interactions consist of electrostatic interactions and Lennard-Jones potentials using Lorentz-Berthelot mixing. The electrode sites Lennard-Jones parameters are the ones of Cl⁻ [21]. The electrolyte consists of an aqueous solution of NaCl composed of 603 extended simple point charge model water molecules [22] and 20 ion pairs [21]. The cross-sectional area is 2.20 nm^2 and the length along the z axis $L_z = 11$ nm.

The simulations were performed with a time step of 2 fs in the NVT ensemble at 298 K using a Nosé-Hoover thermostat with a coupling constant of 0.4 ps. The systems were equilibrated during 10 ns before a production run of 10 ns.

For the finite field simulations, we use the CCS configuration with 3D PBCs. The single electrode, which is made of 12 planes of atoms, is set at null potential and the field E ranges from 0 to 2 V nm⁻¹. For the constant applied
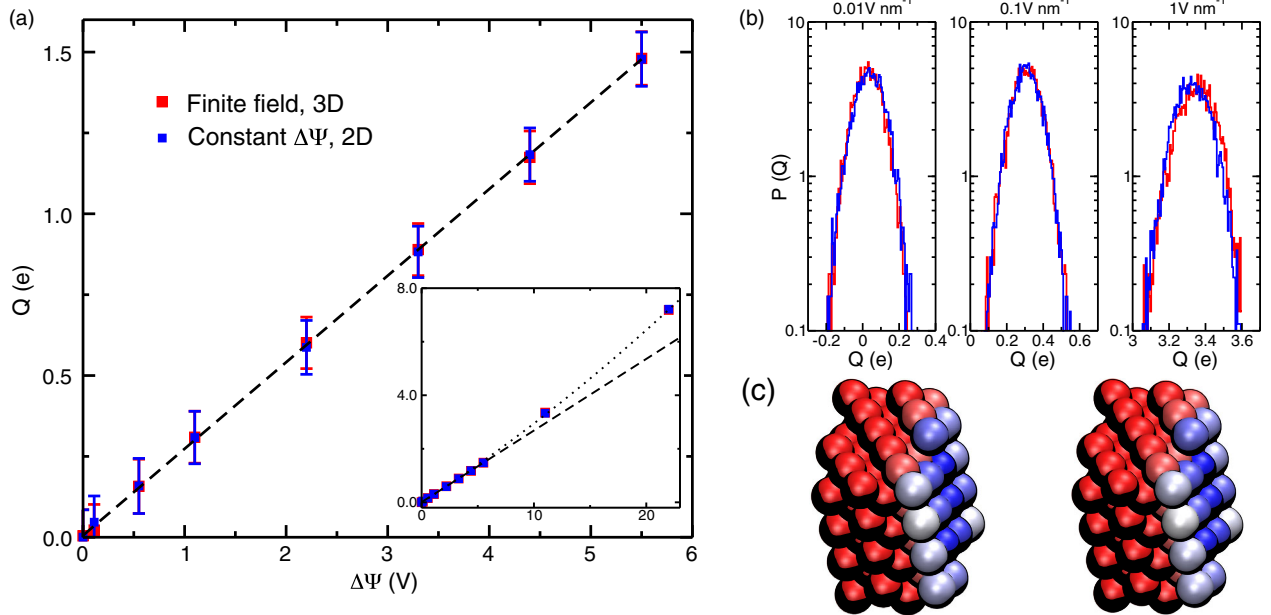

FIG. 2. The single electrode behaves as two distinct constant potential electrodes. (a) Average of the total accumulated charge on the positive side as a function of the applied potential. The error bars correspond to the standard deviation of the charge distribution. (b) Normalized distributions of the instantaneous total charge on the positive half-electrode for various finite electric fields ($E = 0.01$, 0.1, and 1 V nm⁻¹ from left to right, red lines) or the corresponding applied voltages ($\Delta\Psi = 0.11$, 1.1, and 11 V for a cell length of 11 nm from left to right, blue lines). (c) Snapshot of the positive electrode for a finite field of 0.5 V nm⁻¹ (left) and the corresponding applied potential of 5.5 V (right), for the same electrolyte configuration. The atoms are colored according to their instantaneous charge, between 0 e (red) and 0.1 e (blue).

potential simulations, we set up the ECS configuration with 2D PBCs. In this setup the two electrodes are of equal dimensions (i.e., six planes of atoms each), kept under constant potentials Ψ_{left} and Ψ_{right} such that $\Delta\Psi = \Psi_{\text{right}} - \Psi_{\text{left}} = -EL_z$, using the same values for E as above. In both series of simulations, the value of the η parameter for the Gaussian charges has been set to 0.5052 Å^{-1} following Ref. [19]. Electroneutrality is enforced during the charge calculation process [17] (note that a different constraint on the total charge could also be used to simulate non-neutral systems [23]).

A first validation is provided by comparing the polarization of the electrodes with the two setups. To do this we split the single electrode in the CCS setup into two parts. This is easily made since one side accumulates positive charge and the other is exactly opposite, while the center is almost neutral. First, the average accumulated charge Q on the positive side is compared with the ECS setup on Fig. 2(a) for a wide range of applied fields (potentials). The agreement between the two methods is excellent since the points are almost superimposed. This is true not only for voltages up to 6 V where the charge increases linearly with the applied potential (which reflects a constant differential capacitance [16]), but also up to 20 V for which the variation is not linear anymore (see the inset). The probability distributions of the instantaneous values of this quantity [Fig. 2(b)] are also identical, which shows that the two methods sample the same configuration space. Finally, Fig. 2(c) illustrates the instantaneous electrode charges for a given electrolyte configuration. The two systems are indistinguishable, showing that even at the local scale the finite field method yields a correct representation of the electrode-electrolyte interface.
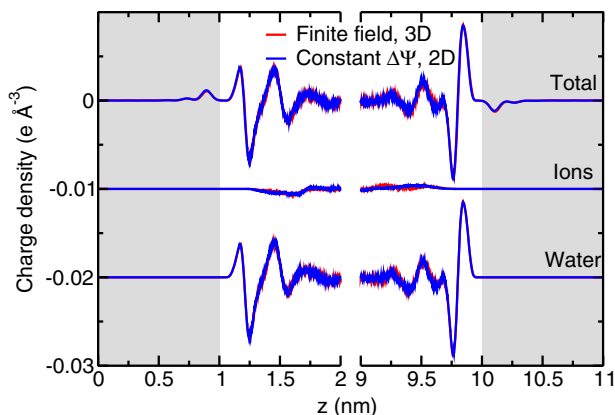

FIG. 3. Charge density within the electrode and the electrolyte for a finite field of 0.1 V nm^{-1} or the corresponding applied potential of 1.1 V. The contributions of water molecules and ions to the total charge distribution are also shown; they were shifted by -0.01 e Å^{-3} for a better readability. The gray-shaded areas correspond to the electrodes (the CCS was translated in order to match with the ECS setup).

When a finite field is applied to a bulk liquid, due to the PBCs the charges cannot accumulate in a specific region so that there is a net electric field in each point of the supercell. Here, the presence of a blocking surface (the electrode) results in the formation of polarized layers on the electrolyte side. The polarization arises from two mechanisms: (i) reorientation of the water molecules; (ii) local charge imbalance by the accumulation of one ionic species and depletion of the other. The structure adopted by the liquid may be compared with the case of constant applied potential simulations. As shown on Fig. 3, the agreement is again very good for the variation of the charge density and its splitting between water and ionic contributions across the simulation cell. The asymmetry of the double layer structure at the two interfaces is also very well reproduced. This validates further the use of the single electrode in order to study electrochemical interfaces using 3D PBCs. Additional tests on the electric field and Poisson potential for several applied voltages are provided in the Supplemental Material [24]; they all show the same level of accuracy.

In conclusion, we have demonstrated the possibility to simulate metal slabs with fluctuating surface charge and in the presence of an explicit electrolyte that counterbalances the charge. This is done through the combination of two methods: an applied finite field which polarizes the cell and a constant potential electrode that screens the field in its bulk, leading to the formation of two independent electrochemical interfaces. The net charge on one electrode surface is the opposite of the net charge on the other, which maintains the overall charge neutrality of the metal slab. The electrode surface charge fluctuations are compensated by the adsorption of ions from the electrolyte. The method is validated through extensive comparisons with simulations using constant applied potential between two separated electrodes (and 2D PBCs). From the practical point of view, it is much easier to implement in classical MD packages since it avoids the introduction of 2D PBCs. From the computational point of view, the method is also more efficient: The simulation time is reduced by approximately 15% (the standard Ewald summation technique was used in both cases for a fair comparison but the 3D PBCs simulations could be even faster by using alternative methods). Last, but not least, it could much more easily be applied to the case of *ab initio* molecular dynamics, which would open the door for the first-principles simulation of electrochemical reactions occurring at electrodes, in the presence of an explicit electrolyte.

*Corresponding author.
mathieu.salanne@sorbonne-universite.fr

[1] F. Calle-Vallejo and M. T. M. Koper, Electrochim. Acta **84,** 3 (2012).

[2] O. M. Magnussen and A. Groß, J. Am. Chem. Soc. **141,** 4777 (2019).

[3] N. Bonnet, T. Morishita, O. Sugino, and M. Otani, Phys. Rev. Lett. **109,** 266101 (2012).

[4] M. M. Melander, M. J. Kuisma, T. E. K. Christensen, and K. Honkala, J. Chem. Phys. **150,** 041706 (2019).

[5] S. Nishihara and M. Otani, Phys. Rev. B **96,** 115429 (2017).

[6] F. Nattino, M. Truscott, N. Marzari, and O. Andreussi, J. Chem. Phys. **150,** 041722 (2019).

[7] J. Le, M. Iannuzzi, A. Cuesta, and J. Cheng, Phys. Rev. Lett. **119,** 016801 (2017).

[8] A. Bouzid and A. Pasquarello, J. Phys. Chem. Lett. **9,** 1880 (2018).

[9] I. Souza, J. Íñiguez, and D. Vanderbilt, Phys. Rev. Lett. **89,** 117602 (2002).

[10] O. Diéguez and D. Vanderbilt, Phys. Rev. Lett. **96,** 056401 (2006).

[11] M. Stengel, N. A. Spaldin, and D. Vanderbilt, Nat. Phys. **5,** 304 (2009).

[12] C. Zhang and M. Sprik, Phys. Rev. B **94,** 245309 (2016).

[13] T. Sayer, C. Zhang, and M. Sprik, J. Chem. Phys. **147,** 104702 (2017).

[14] J. I. Siepmann and M. Sprik, J. Chem. Phys. **102,** 511 (1995).

[15] D. Golze, M. Iannuzzi, M.-T. Nguyen, D. Passerone, and J. Hutter, J. Chem. Theory Comput. **9,** 5086 (2013).

[16] D. T. Limmer, C. Merlet, M. Salanne, D. Chandler, P. A. Madden, R. van Roij, and B. Rotenberg, Phys. Rev. Lett. **111,** 106102 (2013).

[17] T. R. Gingrich and M. Wilson, Chem. Phys. Lett. **500,** 178 (2010).

[18] M. Kawata and M. Mikami, Chem. Phys. Lett. **340,** 157 (2001).

[19] S. K. Reed, O. J. Lanning, and P. A. Madden, J. Chem. Phys. **126,** 084704 (2007).

[20] J.-M. Caillol, J. Chem. Phys. **101,** 6080 (1994).

[21] I. S. Joung and T. E. Cheatham, J. Phys. Chem. B **112,** 9020 (2008).

[22] H. J. C. Berendsen, J. R. Grigera, and T. P. Straatsma, J. Phys. Chem. **91,** 6269 (1987).

[23] A. Levy and M. Z. Bazant, arXiv:1905.05789.

[24] See Supplemental Material at http://link.aps.org/supplemental/10.1103/PhysRevLett.123.195501 for additional tests on the electric field and Poisson potential for several applied voltages.